# Fe-Sulfide Liberation and Association as a Proxy for the Interpretation of Acid Rock Drainage (ARD) Test Results

Olga Guseva[1], Alexander K. B. Opitz[1], Jennifer L. Broadhurst[1], Susan T. L. Harrison[1,2], Dee J. Bradshaw[1], Megan Becker[1,3]

[1]*Minerals to Metals Initiative, University of Cape Town, South Africa, gsvolg001@myuct.ac.za*

[2]*Centre for Bioprocess Engineering Research, University of Cape Town, South Africa*

[3]*Centre for Minerals Research, University of Cape Town, South Africa*

## Abstract

Acid rock drainage (ARD) characterisation and prediction protocols, comprising geochemical static, kinetic and biokinetic tests, sometimes fail to adequately assess the ARD potentials of sulfidic mine wastes. Several authors have partly linked this shortfall to the insufficient use of mineralogical and textural analyses. Mineral liberation and association data may inform the interpretation of the results of standard ARD tests and this study assesses these parameters for Fe-sulfide minerals in the feed material for humidity cell (meso-scale), static and biokinetic (micro-scale) tests. Results show that the dominating textural parameters on the meso- and micro-scales are association and liberation, respectively.

**Keywords:** mineralogy, texture, association, liberation, kinetic tests

## Introduction

Acid rock drainage (ARD) occurs through complex mechanisms of acid formation and neutralisation reactions associated with metal sulfide oxidation and gangue mineral dissolution, respectively. The processes result in acidic drainage that often contains elevated levels of toxic elements. Due to its abundant occurrence with valuable minerals, pyrite is typically recognized as the main mineral contributing to ARD formation from mine wastes; however, it is well recognized that all mineral sulfides may be oxidized in the presence of oxygen and water (Nordstrom and Alpers 1999; INAP 2012). Mining and processing activities produce waste material ranging from coarse rocks to fine tailings. These waste fragments have a larger combined surface area exposed to oxidative conditions than the original undisturbed rock, exacerbating any naturally occurring ARD.

ARD characterisation and prediction techniques typically include a suite of geochemical static and kinetic tests (INAP 2012; Parbhakar-Fox and Lottermoser 2015). Static tests are relatively quick and inexpensive and are routinely performed on finely milled subsamples (particles passing 75µm) of the parent material, where the minerals are assumed to be fully liberated from one another. This accelerates reaction kinetics to gain an indication of the "worst case" scenario for ARD generation. In doing so, any textural relationships between acid forming and neutralizing minerals are destroyed (Brough et al. 2017). Kinetic tests (mainly humidity cell tests) are costlier and more time consuming, and are thus not explicitly performed on every sample, rather on those yielding uncertain or conflicting results in the characterisation stages. A coarser particle size distribution (particles passing 6.3mm) is used to provide an indication of the long-term weathering behaviour (Lengke et al. 2010; ASTM 2013). At this scale, textural and mineralogical relationships are thought to still be retained. As none of the above tests address the contribution made by naturally occurring microorganisms to ARD formation, the University of Cape Town (UCT) biokinetic test (Hesketh et al. 2010) was developed and makes use of finely milled material (passing 150µm).

Although recommended (Parbhakar-Fox et al. 2011; Becker et al. 2015; Brough et al. 2017; Dold 2017), thorough mineralogical and textural analyses are rarely undertaken

for ARD assessment due to associated time and cost constraints (Jamieson et al. 2015). Textural factors influencing ARD formation include the grain size distributions, associations, reactivity, and the degree of liberation of the acid forming and neutralizing mineral phases present (Parbhakar-Fox et al. 2011) and may be assessed on three general scales, namely macro-, meso- and micro-texture. These scales may be linked to particle size, which has been found to affect metal recovery and drainage kinetics in heap leach systems due to the dependence of particle surface area on reactivity (Ghorbani et al. 2011). Finer particles consisting solely of the leachable material have been found to have an increased potential for reactivity as opposed to coarser particles where the leachable material was encapsulated (Ghorbani et al. 2011; Fagan-Endres et al. 2017). Liberation of minerals refers to mineral exposure to the reactive environment and may be classed into liberated, unliberated and locked/encapsulated categories (Evans and Morrison 2016). For humidity cell tests liberated material has been found to be more likely to produce acidic leachate than material with a lower degree of liberation (Brough et al. 2017). This phenomenon is well described in heap bioleaching studies (Fagan-Endres et al. 2017).

Mineralogy and textural analyses assess the mineral liberation, grade of a sample, mineral shape, size and interrelationships within the particles. A variety of tools exist for quantifying these parameters (Becker et al. 2016), but one that is frequently used is automated scanning electron microscopy with energy dispersive spectrometry (e.g. QEMSCAN, MLA, Mineralogic, TIMA). Challenges do still exist when quantifying textural measurements as there are no strict guidelines for quantitative texture in ARD test work. Representative sampling, quantifying the statistical implications thereof, obtaining the required number of particles of interest, as well as other factors associated specifically with two-dimensional measurements, are often overlooked or not fully quantified. Qualitative textural assessment is also frequently performed. The acid rock drainage index (ARDI) considers the texture and mineralogy for ARD formation through parameters such as sulfide content, associations, morphology, alteration (extent of weathering), and neutralising mineral content and association with sulfide minerals. It was developed as a semi-quantitative segment of a geometallurgy-mineralogy-texture (GMT) approach and was designed for the provision of rapid estimates of ARD potential for whole-rock samples at mine sites (Parbhakar-Fox et al. 2011).

Thorough mineralogical analyses and an awareness of mineral liberation and association may improve the interpretation of contradictory or unexpected results obtained from commonly used static and kinetic tests (Brough et al. 2013). The current study aims to assess the dominating textural parameters on the particle size scale of static and biokinetic tests (micro-scale) and humidity cell tests (meso-scale). Quantitative textural data is used to assess Fe-sulfide association and liberation on these scales, and potential implications of these results is addressed in the context of humidity cell test work for the meso-scale, interlinked with results published in Opitz et al. (2016) for the micro-scale.

## Methods

This study was performed using a waste rock sample generated from the mining of a greenstone gold deposit. The static and biokinetic test feed material preparation is described in Opitz et al. (2016) and will be referred to as the standard characterisation test (SCT) feed. The meso-scale humidity cell test (HCT) feed material was prepared as per the ASTM D5744-13 method (ASTM 2013). Feed material larger than 150 µm was dry-screened, while material smaller than 150 µm was wet-screened to minimise particle agglomeration. Presentation of the results of the HCT feed material was split into six size fractions, while the SCT material is presented as the bulk.

Textural data was obtained using a FEI QEMSCAN 650F instrument with two Bruker XFlash 6130 detectors at the University of Cape Town. Suitably representative subsamples were obtained using eight- and ten-way rotary sample dividers and prepared into polished sample blocks for analysis. Standard blocks (30mm diameter) were prepared as vertical sections for all material smaller than 1mm. To allow for the measurement of sufficient particles of interest, HCT sample fractions larger than 1mm were prepared as

70×70mm square blocks. When analysing the data obtained from QEMSCAN, categorisers were set up to obtain the number of Fe-sulfide-bearing particles, Fe-sulfide grain size distribution, association and liberation data for the SCT and HCT feed material. Liberation categories were defined as liberated (>90% particle area for mineral of interest) and unliberated (< 90% particle area for mineral of interest).

## Results

A pre-existing data set exists for the sample used in this study. Results for static and biokinetic tests, as well as the ARDI, mineralogical ANC and bulk mineralogy obtained via QEMSCAN are presented in Opitz et al. (2016), sample B. For the purposes of this study the pyrite and pyrrhotite were grouped into a general Fe-sulfide category, with other minerals being grouped into categories based on their relative reactivity as given by Lawrence and Scheske (1997). Bulk mineralogy indicated the dominance of pyrite in the Fe-sulfide category, while the dissolving, fast, intermediate and slow weathering, inert and other categories were dominated by calcite, olivine, biotite, plagioclase feldspar, quartz and apatite, respectively.

Table 1 shows the Fe-sulfide content and liberation of the sample by size for the HCT (columns 1-6) and SCT (column 7) feed material (as the bulk). Row one defines the Fe-sulfide content of each fraction as a percentage of the total Fe-sulfide content of the sample, for example, column 1 shows that 62% of all the Fe-sulfide present in the HCT feed is concentrated in the -6700/+2000μm size fraction. In column 7, however, the Fe-sulfide content and liberation are presented as the bulk, with the SCT feed having a total Fe-sulfide content of 7%. Rows two and three show the liberation of Fe-sulfide material, with the percentages representing the amount of liberated material (row two) and unliberated material (row three) in that size fraction. Fe-sulfides in the HCT feed predominantly occur as unliberated particles, with more than 50% of Fe-sulfides in size fractions greater than 425μm being unliberated and mineral association dominating over liberation (see Figure 2). For the SCT feed the liberation of the Fe-sulfide material is the dominating textural parameter, with only 10% unliberated Fe-sulfides.

Figure 1 below presents the corresponding false colour images for the size fractions listed in Table 1 and serves only as a visual representation of the Fe-sulfide-bearing particles that fall into the liberated and unliberated categories.

Figure 2 shows the Fe-sulfide liberation and association by size for the HCT feed and the bulk for the SCT feed material (see also Table 1). Fe-sulfide liberation increases as particle size decreases, with negligible Fe-sulfide liberation at size fractions above 1000μm, inferring unliberated texture (association dominated). The increase in liberation with size fraction is prominent for size fractions smaller than 1000μm, due to the largest Fe-sulfide grains not exceeding 600μm and the finest grains being under 3μm. Nonetheless, a small amount of liberated material does appear in the -1400/+1000 fraction, due to the massive sulfide texture. Fe-sulfide mineral association in all size fractions is dominated by inert, slow weathering and intermediate weathering material, followed by notably smaller associations to carbonate, fast weathering and other sulfides. The Fe-sulfide asso-

***Table 1*** *Row one: distribution by size represented as a percentage of the total Fe-sulfide in the sample (column 7 represented as the bulk). Rows two and three: Fe-sulfide liberation by size, with the percentages showing the portion of the Fe-sulfide in that fraction that is liberated or unliberated. Liberation for Fe-sulfide material is defined as liberated when 90% or more of its area is exposed to no other minerals and unliberated as having more than 90% of its area surrounded by other minerals. The size fractions of the HCT feed are 1: -6700/+2000; 2: -2000/+1400; 3: -1400/+1000; 4: -1000/+425; 5: -425/+150; 6: -150/+0 μm; and 7: SCT bulk feed (-150μm)*

| Sample | 1 | 2 | 3 | 4 | 5 | 6 | 7 |
|---|---|---|---|---|---|---|---|
| Fe-sulfide | 62% | 6% | 6% | 7% | 6% | 13% | 7% |
| Liberated | 0% | 0% | 3% | 18% | 48% | 81% | 90% |
| Unliberated | 100% | 100% | 97% | 82% | 52% | 19% | 10% |

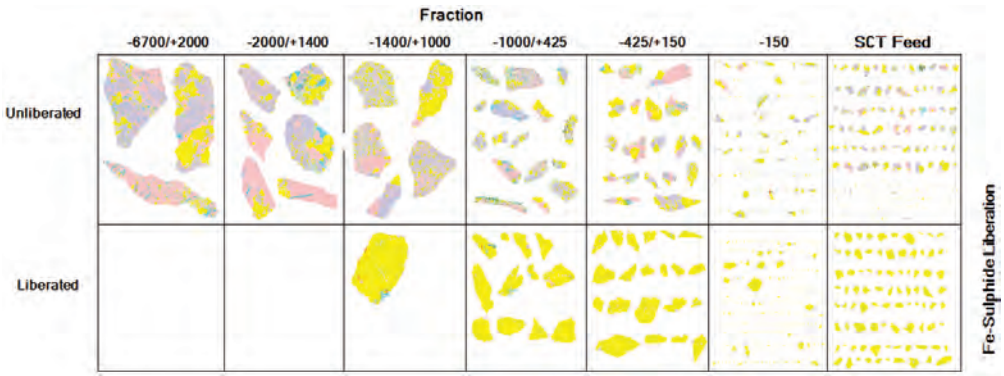


*Figure 1 QESMCAN Image Grid categoriser set up by size fraction for Fe-sulfide-bearing particles. False colour images of Fe-sulfide-bearing particles correspond to the size fractions provided in Table 1. See Figure 2 for colour legend. The images are meant only to provide a visual representation of the Fe-sulfide liberation throughout size fractions and do not serve to display the relative abundance of particles in the categories or represent the "average" particle in each size fraction.*

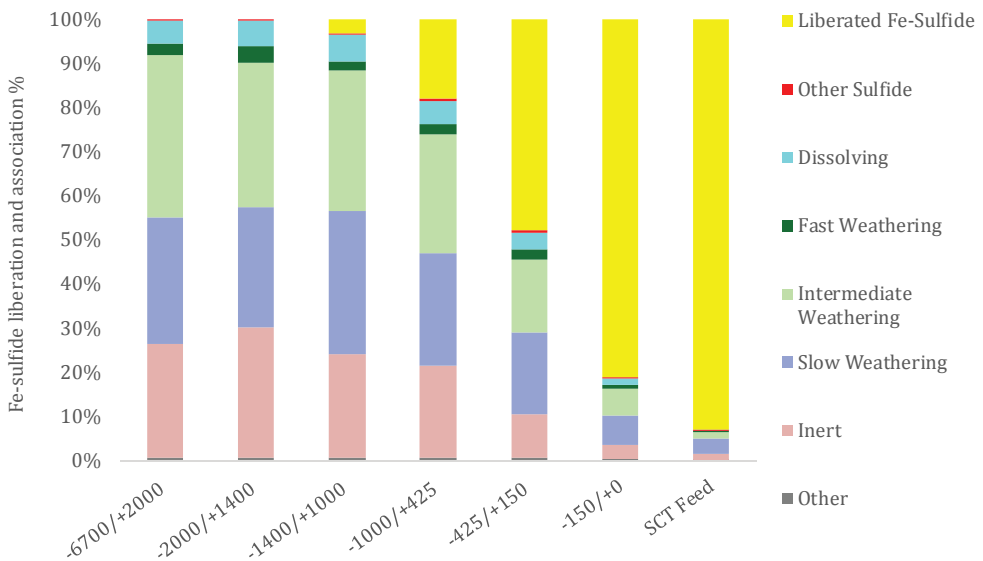


*Figure 2 Fe-sulfide liberation and association for HCT and SCT feed material. The HCT feed is presented by size, while the SCT material is presented as the bulk. The major minerals contributing to the sub-groups are: Fe-Sulfide: pyrite, pyrrhotite; Other Sulfide: chalcopyrite, galena, sphalerite; Dissolving: calcite, dolomite, ankerite; Fast Weathering: olivine, diopside; Intermediate Weathering: epidote, pyroxene, amphiboles, chlorite, biotite; Slow Weathering: albite, orthoclase, muscovite; Inert: quartz, sphene; Other: apatite*

ciation for the SCT feed is considerably lower than for the HCT feed material given the high liberation, but the unliberated material still shows Fe-sulfide association dominated by slow weathering, intermediate weathering and inert material.

## Discussion

Liberated material comprises most of the Fe-sulfide mineral category in the SCT feed, as is expected for finely milled material. Consequently, this Fe-sulfide material is accessible for reaction under static and biokinetic test conditions. The very small association of Fe-sulfides with carbonate minerals indicates that the carbonate minerals may be liberated or associated with other phases. Static test results (Opitz et al. 2016) characterise the sample as potentially acid forming, which is expected as the Fe-sulfide content is compar-

atively larger (and predominantly liberated) than the dissolving mineral content. The biokinetic test results show a circumneutral final pH for this sample, which may be explained by reaction of the (potentially liberated) carbonate material, resulting in an initial rise in test pH to pH 7.0. Such conditions would hinder microbial metabolism and remove soluble ferric iron from solution, as may be observed by the corresponding low redox potential profile for sample B (Opitz et al. 2016).

The HCT feed association and liberation characteristics will have implications for humidity cell test results, as material that is liberated is readily susceptible to oxidizing conditions and will generate acidic leachate more rapidly than unliberated material (Brough et al. 2017). On this scale, most of the Fe-sulfide material is concentrated in size fractions above 1000µm, where association with intermediate weathering, slow weathering and inert mineral phases dominates. More than 70% of the Fe-sulfide material is found in size fractions above 1000µm (more than 90% of Fe-sulfides unliberated), thus the leaching behaviour of the HCT is likely to be dictated by this material. The Fe-sulfide material in the unliberated fraction, where it may be partially exposed, would still be accessible to oxidative conditions but a significantly longer time frame would be required to leach the Fe-sulfide grains completely, as opposed to more rapid leaching for liberated grains. This could have implications for the minimum specified duration for standard humidity cell tests (20 weeks) (ASTM 2013). Considering the potentially longer leach times due to predominantly unliberated material, it is expected that a longer test duration would be required for this sample to enable collection of meaningful leachate data. Additionally, the inert material associated with unliberated Fe-sulfides will not be susceptible to short-term weathering under the circum-neutral pH conditions within the humidity cell experiments. Physical breakage would be required to access these sulfides completely. Intermediate and slow weathering phases, however, would react over time and potentially expose the associated Fe-sulfide material to the oxidising environment, making acid formation over a longer period possible. Acid forming and neutralising minerals could also still be accessed through minor cracks or pores within the particles, but the net ARD formation from this pathway would be limited by mass transfer effects (Ghorbani et al. 2011). Fe-sulfide association with carbonate material may allow acid formed from these grains to be neutralised locally but the carbonate content is very small and would not offer sufficient neutralising capacity to label this sample as net non-acid forming, as shown by static test results (Opitz et al. 2016).

## Conclusions

The Fe-sulfide material in the SCT feed was well liberated (dominating textural parameter), as expected for the determination of the "worst case" scenario for acid formation and neutralisation. For humidity cell tests the Fe-sulfide material in this sample is concentrated in the coarse size fractions where it is unliberated and associated predominantly with intermediate and slow weathering phases, which will not readily weather under circumneutral pH conditions. Over time these phases may weather, however, exposing the Fe-sulfide material. Fe-sulfides are also largely associated with inert minerals, making them accessible only through the exposed area in these unliberated categories or via minor cracks/pores. This will potentially extend the humidity cell test duration. Association of the Fe-sulfides with dissolving phases may offer local acid neutralisation but will be insufficient to buffer acid formation over time.

The knowledge gained from thorough textural and mineralogical analyses of waste samples could allow for an improved understanding of laboratory-based geochemical test results. This improvement will enable better characterisation and prediction of the ARD potential within waste deposits, and ultimately aid in the creation of reliable and accurate modelling frameworks.

## Acknowledgements

Grateful thanks to the staff in the Department of Chemical Engineering at UCT who assisted with the mineralogical analyses. This work is based on the research supported in part by the National Research Foundation of South Africa (Grant Numbers 86054). The opinions, findings and conclusions or recommendations expressed in any publication

generated by the NRF supported research is that of the author(s), and that the NRF accepts no liability whatsoever in this regard. This project is supported in part by the Water Research Commission (Project K5/2846/3).

## References

ASTM (2013) Standard Test Method for Laboratory Weathering of Solid Materials Using a Humidity Cell. D5744-13 1–23. doi: 10.1520/D5744-13E01.2

Becker M, Dyantyi N, Broadhurst JL, et al (2015) A mineralogical approach to evaluating laboratory scale acid rock drainage characterisation tests. Miner Eng 80:33–36. doi: http://dx.doi.org/10.1016/j.mineng.2015.06.015

Becker M, Wightman EM, Evans CL (eds) (2016) Process Mineralogy: JKMRC Monograph Series in Mining and Mineral Processing: No. 6. Julius Kruttschnitt Mineral Research Centre, The University of Queensland, Queensland, Australia

Brough C, Strongman J, Bowell R, et al (2017) Automated environmental mineralogy; the use of liberation analysis in humidity cell testwork. Miner Eng 107:112–122. doi: 10.1016/j.mineng.2016.10.006

Brough CP, Warrender R, Bowell RJ, et al (2013) The process mineralogy of mine wastes. Miner Eng 52:125–135. doi: 10.1016/j.mineng.2013.05.003

Dold B (2017) Acid rock drainage prediction: A critical review. J Geochemical Explor 172:120–132. doi: 10.1016/j.gexplo.2016.09.014

Evans CL, Morrison RD (2016) Process Mineralogy: JKMRC Monograph Series in Mining and Mineral Processing: No. 6. In: Becker M, Wightman EM, Evans CL (eds)

Fagan-Endres MA, Cilliers JJ, Sederman AJ, Harrison STL (2017) Spatial variations in leaching of a low-grade, low-porosity chalcopyrite ore identified using X-ray μCT. Miner Eng 105:63–68. doi: 10.1016/j.mineng.2017.01.010

Ghorbani Y, Becker M, Mainza A, et al (2011) Large particle effects in chemical/biochemical heap leach processes - A review. Miner Eng 24:1172–1184. doi: 10.1016/j.mineng.2011.04.002

Hesketh AH, Broadhurst JL, Bryan CG, et al (2010) Biokinetic test for the characterisation of AMD generation potential of sulfide mineral wastes. Hydrometallurgy 104:459–464. doi: 10.1016/j.hydromet.2010.01.015

INAP (2012) Global Acid Rock Drainage Guide , INAP: The International Network for Acid Prevention

Jamieson HE, Walker SR, Parsons MB (2015) Mineralogical characterization of mine waste. Appl Geochemistry 57:85–105. doi: 10.1016/j.apgeochem.2014.12.014

Lengke MF, Davis A, Bucknam C (2010) Improving management of potentially acid generating waste rock. Mine Water Environ 29:29–44. doi: 10.1007/s10230-009-0097-1

Nordstrom DK, Alpers CN (1999) Geochemistry of acid mine waters. Environ Geochemistry Miner Depos 6:133–160

Opitz AKB, Becker M, Broadhurst JL, et al (2016) The Biokinetic Test as a Geometallurgical Indicator for Acid Rock Drainage Potentials. Perth, Australia, pp 183–191

Parbhakar-Fox A, Lottermoser BG (2015) A critical review of acid rock drainage prediction methods and practices. Miner Eng 82:107–124. doi: 10.1016/j.mineng.2015.03.015

Parbhakar-Fox AK, Edraki M, Walters S, Bradshaw D (2011) Development of a textural index for the prediction of acid rock drainage. Miner Eng 24:1277–1287. doi: 10.1016/j.mineng.2011.04.019